

In-situ strain analysis of potential habitat composites exposed to a simulated long-term lunar radiation exposure

Kristina Rojdev^{a,b,*}, Mary Jane E. O'Rourke^a, Charles Hill^a, Steven Nutt^c, William Atwell^d

^a NASA-Johnson Space Center, 2101 NASA Parkway, Houston, TX 77058, USA

^b University of Southern California, 854B Downey Way, Los Angeles, CA 90089, USA

^c University of Southern California, 3651 Watt Way, VHE 406, Los Angeles, CA 90089, USA

^d The Boeing Company, 13100 Space Center Blvd., HB 2-30, Houston, TX 77059, USA

ARTICLE INFO

Available online 7 June 2012

Keywords:

Composites

Proton

Radiation

Strain

Crosslinking

Scission

ABSTRACT

NASA is studying the effects of long-term space radiation on potential multifunctional composite materials for habitats to better determine their characteristics in harsh space environments. Two epoxy-matrix composite materials were selected for the study and were mounted in a test stand that simulated the biaxial stresses of a pressure vessel wall. The samples in the test stand were exposed to radiation at fast (0.1478 krad/s) and slow (0.0139 krad/s) dose rates, and the strain and temperature were recorded during the exposure. During a fast dose rate exposure, negative strain was recorded, decreasing with time, an indication of matrix shrinkage. Given previous radiation studies of polymers, this is expected to be a result of radiation-induced crosslinking in the epoxy matrix. However, with a slow dose rate, the materials exhibited a positive strain that increased with time, corresponding to stretching of the materials. This result is consistent with scission or degradation of the matrix occurring, possibly due to oxidative degradation.

Published by Elsevier Ltd.

1. Introduction

One of NASA's missions is to continue to explore space beyond Low Earth Orbit (LEO) by focusing on technologies that will advance the state of the art and provide for longer duration missions. One area of interest is long-term surface habitation, which requires large structures situated in harsh environments for extended periods of time. These large structures must be lightweight and multifunctional in nature. Thus, polymeric composites have gained interest as a potential structural material for surface habitation. However, there are several unknowns in using composite materials in a space environment, particularly a long-term radiation environment. To better understand this problem, NASA is studying the effects of long-duration radiation exposure on potential multifunctional composite materials for habitats. The strain and temperature response of two composite materials during radiation exposure and bi-axial stress, simulating a habitat on the lunar surface during a long-duration exposure to radiation, will be discussed.

1.1. Assumptions

In performing this work, certain assumptions were required to make the study feasible. This work assumes a habitat is on the lunar surface and a service life of 30 years. Although the lunar surface is chosen for this study, any planetary surface with limited atmosphere and magnetic field would be applicable with regard to the radiation environment. In addition, we assume a pressurized habitat containing air at an elevated oxygen concentration, and no shielding from the radiation environment on the exterior. Finally, it is assumed that the habitat is exposed to one very large solar particle event (SPE) during each solar cycle, as well as a constant galactic cosmic ray (GCR) exposure.

1.2. Space radiation environment

There are two primary forms of space radiation that are of concern for materials: Solar Particle Events (SPE) and Galactic Cosmic Rays (GCR). The SPEs emanate from the sun, which follows an 11-year solar cycle. During a period known as solar maximum, the sun tends to have more SPEs than during solar minimum. These SPEs range in intensity and in frequency, as shown in Fig. 1.

The GCRs are high-energy radiation penetrating the heliosphere from outside the solar system. Every element in the periodic table is included in the GCR particles, and protons are

* Corresponding author at: NASA-Johnson Space Center, 2101 NASA Parkway, Houston, TX 77058, USA.

E-mail addresses: kristina.rojdev-1@nasa.gov, rojdev@usc.edu (K. Rojdev), MaryJane.E.O'Rourke@nasa.gov (M.J.E. O'Rourke), charles.s.hill@nasa.gov (C. Hill), nutt@usc.edu (S. Nutt), william.atwell@boeing.com (W. Atwell).

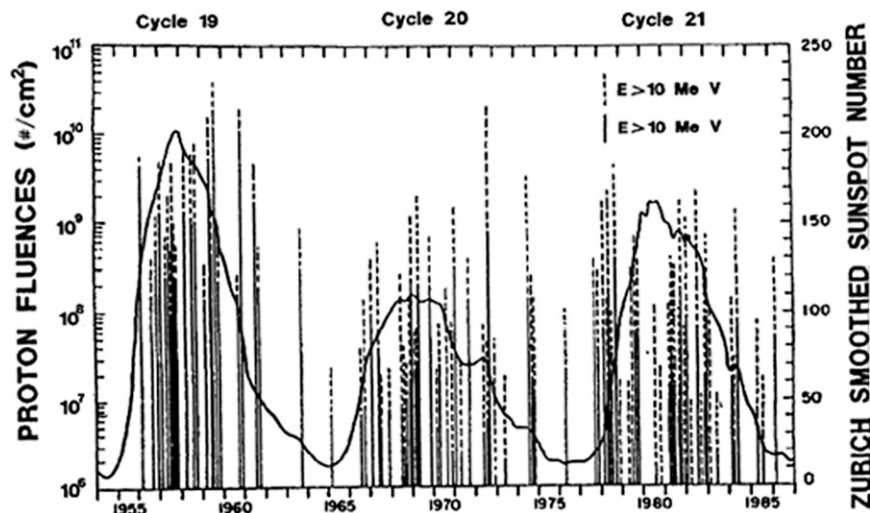


Fig. 1. Solar events for cycles 19–21 (NASA-STD-3000).

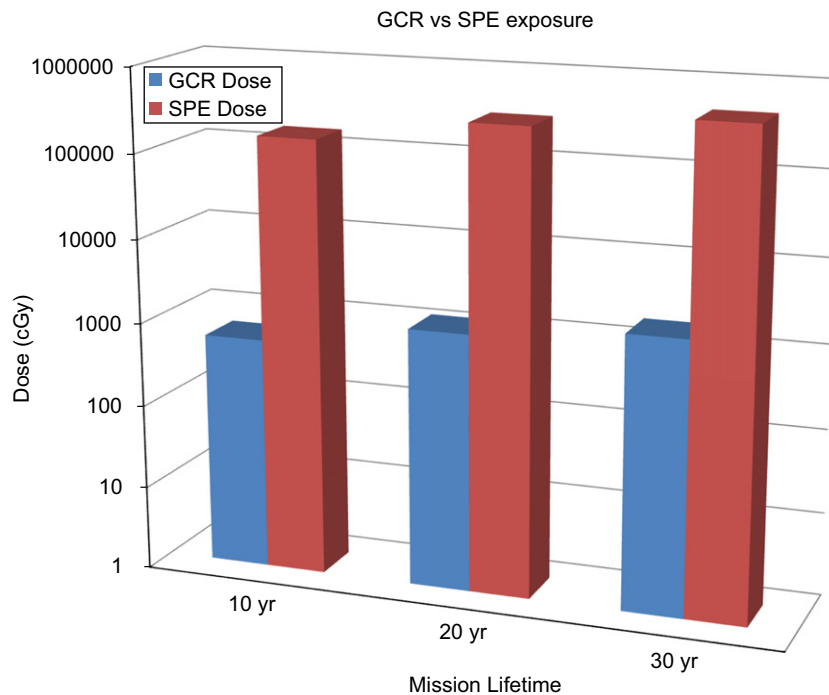


Fig. 2. The dose accumulated by a material completely exposed to a surface environment.

the most abundant. However, the concern with GCRs typically results from the prevalence of heavy ions, such as iron ions. Unlike SPEs, the GCRs are an ever-present background radiation and are isotropic within the solar system, yet they are still modulated by the solar cycle such that the GCR intensity is greatest during solar minimum.

1.3. Preliminary environmental modeling

To better understand the environment in which these materials would be deployed, and to develop a baseline for the experimental radiation, some initial modeling was performed. In Fig. 2, the absorbed dose on a material from GCRs versus SPEs was compared, showing that the majority of absorbed dose is a result of SPE exposure. Thus, the following study focused on proton radiation with characteristics similar to that of an SPE. In Fig. 3, the absorbed doses for three different mission lengths are

compared. The total absorbed dose displayed in this figure is the sum of the GCR exposure and the SPE exposure, which is then multiplied by a safety factor of ten. The factor of safety is introduced to account for any additional SPE exposure that might occur during the solar cycle, and is not necessarily an exceptionally large SPE. For the worst case scenario, a 30-year mission would encounter approximately 500,000 cGy of exposure, based on these calculations.

1.4. Habitation calculations

The internal pressure environment of the habitat set by NASA in conjunction with the lunar environment has specific design implications for the habitat (Jablonski and Ogden, 2008). Because of the absence of an atmosphere on the lunar surface and the internal pressure of the habitat, the predominant stress on the habitat while on the lunar surface is the internal pressure. This

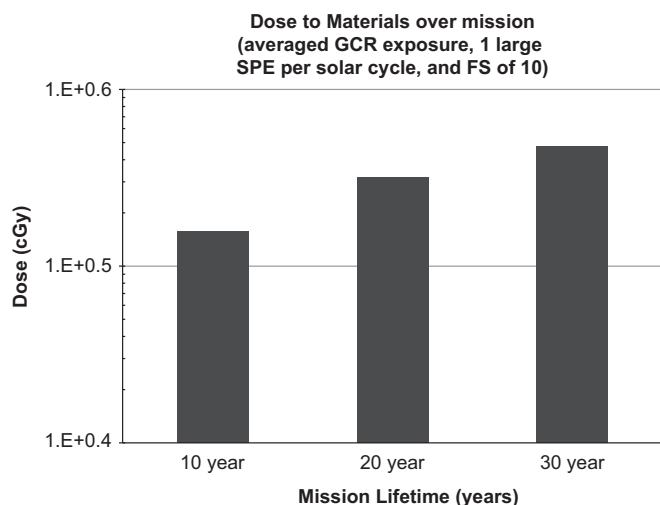


Fig. 3. The total absorbed dose for three different mission lengths.

stress is manifested as biaxial tensile stress on the pressure vessel wall. Therefore, to consider a realistic worst-case scenario, a skin-stiffened laminate was selected to represent the habitat shell. Given the minimum gage thickness of a skin-stiffened structure (Dorsey et al., 2008) and using the calculations for normal and hoop stress on a pressure vessel, the worst case stress imparted to a cylindrical habitat due to internal pressure was calculated to be approximately 41 MPa.

2. Experimental

2.1. Materials

Two materials were selected for this study. The first material is a pre-impregnated composite comprised of carbon fibers (CF, Hexcel IM7) and a toughened-epoxy resin (Cycom 977-3). The second material is a pre-impregnated composite from Specialty Materials, Inc. consisting of 100- μ m boron fibers (BF) and carbon fibers (CF, MR40) impregnated with a toughened-epoxy resin (Newport 301). All samples were manufactured in-house with a quasi-isotropic layup design of [+60/-60/0]_s. The CF-epoxy samples were cured in an autoclave, whereas the BF-CF-epoxy samples were cured in a press. Both methods followed the recommended cure cycles provided by the manufacturers.

2.2. Test setup

Prior to radiation exposure, the samples were placed in a test stand that provided bi-axial tension. In addition, a bi-axial strain gauge was placed on the center of the sample and a thermocouple was placed close to the strain gauge. The strain gauge leads and some of the thermocouples were connected to a data acquisition system (National Instruments). Additional thermocouples were connected to hand-held readers placed in the radiation beam room. Web cameras were used to acquire the readings from the hand-held readers. The data that was collected during the radiation exposures included the change in strain in both directions of the sample and temperature of the sample surface.

2.3. Radiation exposures

All samples were exposed to a total dose of 500 krad using 200 MeV protons. Samples were either exposed to a fast dose rate

Table 1

Description of radiation exposures conducted.

Exposure #	Dose rate	# of Samples	Material
Exposure 1	Slow	5	BF-CF
Exposure 2	Slow	5	CF
Exposure 3	Fast	1	CF
Exposure 4	Fast	1	CF
Exposure 5	Slow	4	2-BF-CF, 2-CF
Exposure 6	Fast	4	2-BF-CF, 2-CF

Table 2

Coefficient of thermal expansion used in thermal strain calculations for each material.

Material	CTE
Aluminum	$1.31\text{E}-5\text{ }^{\circ}\text{F}^{-1}$
CF-epoxy	$1.925\text{E}-6\text{ }^{\circ}\text{C}^{-1}$
BF-CF-epoxy	$4.79\text{E}-6\text{ }^{\circ}\text{C}^{-1}$

of 0.1478 krad/s or a slow dose rate of 0.0139 krad/s. The exposures were performed at Indiana University Cyclotron Facility.

There were a total of six exposures completed for these experiments. All the samples for each exposure were stacked in front of the radiation beam. Table 1 shows the conditions for each exposure.

2.4. Calculations of material strain due to thermal changes

Considering both the temperature data with the strain data collected for each sample revealed that the temperature trends for each exposure were similar to the strain trends of the respective exposures. Thus, calculations were carried out to compare thermal strains with the strain data collected during the radiation exposures.

First, the thermal strain change of the material sample was calculated, using the following equation. Here, α_{lam} is the coefficient of thermal expansion for the material sample and ΔT is the change in temperature.

$$\Delta_{\text{Strain, lam}} = \alpha_{\text{lam}} \Delta T$$

The thermal strain change of the test stand was calculated next. The outer ring of the test stand was made of aluminum, and the equation for the test stand is shown below. Here, α_{Al} is the coefficient of thermal expansion for the aluminum frame and ΔT is the change in temperature.

$$\Delta_{\text{Strain, Al}} = \alpha_{\text{Al}} \Delta T$$

The values used for the coefficients of thermal expansion are shown in Table 2.

After these two calculations were completed, the change in strain between the two equations was compared, and the greater value was assumed to be the driving force for the strain measurements observed. These calculations were then compared with the change in strain measured on the samples during radiation exposure.

3. Results

3.1. Fast dose rate samples

The samples that were exposed to a fast dose rate were part of Exposures 3, 4, and 6. All of the samples in each of these exposures showed an overall decrease in strain with respect to

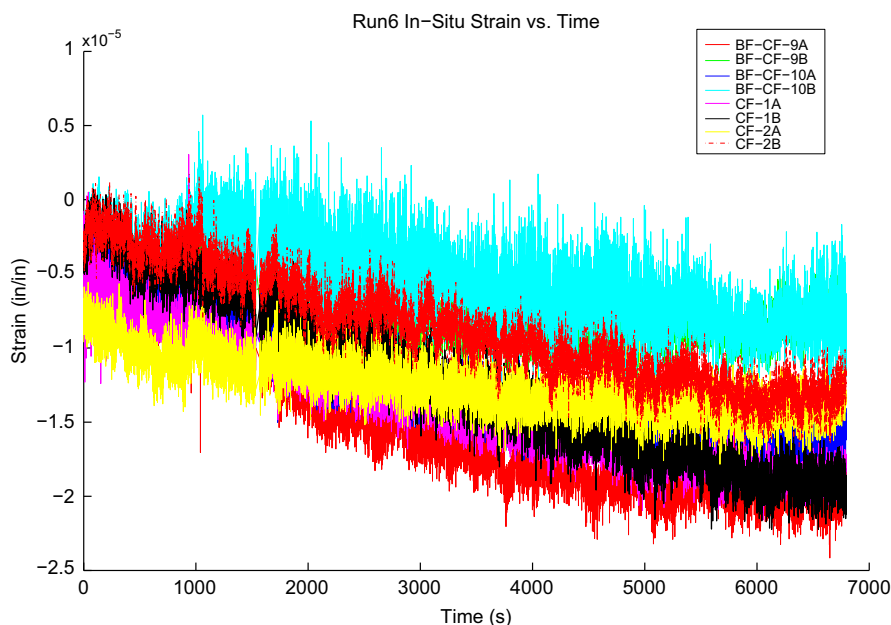


Fig. 4. Measured strain data from Exposure 6, example of a fast dose rate in-situ strain response.

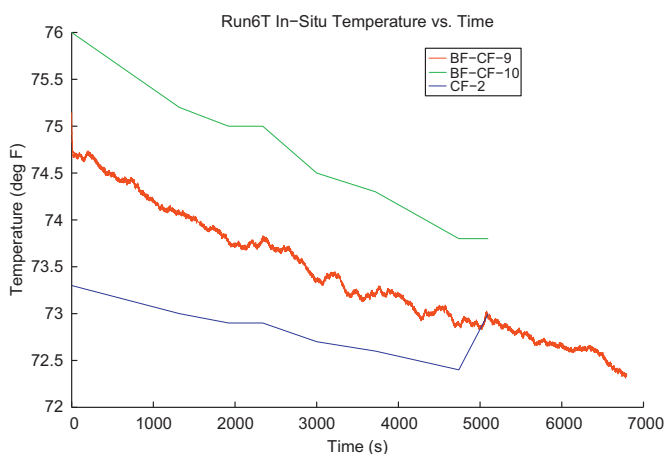


Fig. 5. Measured temperature data from Exposure 6.

time, in both axes. Using Exposure 6 as an example, the decreasing strain was apparent in both materials, as shown in Fig. 4. In Fig. 5, the corresponding temperature data collected for these materials is shown. Both of these graphs correspond to data collected during Exposure 6 in which two BF-CF-epoxy samples (BF-CF-9 and BF-CF-10) were stacked with two CF-epoxy samples (CF-1 and CF-2). In the temperature data, CF-1 did not get recorded due to a hardware malfunction.

3.2. Slow dose rate samples

In Exposures 1, 2, and 5, samples were exposed to a slow dose rate. These samples showed strain increasing with time. Using Exposure 1 as an example, Fig. 6 shows several BF-CF-epoxy samples with an increased strain with respect to time in both axes, followed by a gradual leveling out of the data towards the latter part of the exposure. In this plot, two dashed lines do not follow the rest of the data and correspond to data recorded from BF-CF-6B and BF-CF-11B. These two axes did not record any strain data for Exposure 1, most likely due to software and hardware failures from radiation exposure to the data acquisition

system. The corresponding temperature data for these samples are shown in Fig. 7.

4. Discussion

In this study, samples exposed to a fast dose rate exhibited a decrease in strain with respect to time, whereas those exposed to a slow dose rate exhibited an increase in strain with respect to time. The temperature profiles of the respective samples followed a similar trend of increasing slope in temperature versus time with a slow dose rate and decreasing slope of temperature versus time with a fast dose rate. To verify that the strain observed in the composite samples was not thermally induced, thermal expansion calculations of the aluminum test stand frame and the composite samples were performed and compared. If the measured strain were thermally induced, and if the calculated thermal expansion of the aluminum frame was greater than the calculated thermal expansion of the composite sample, we expected the measured strain to match the calculated thermal expansion of the aluminum frame. Overall, this was not found to be the case. Other potential sources of error include any possible radiation effects on the strain gauges and/or bonding agent used to affix these to the samples. To assess any inaccuracies in the measurements induced by these possible effects, measurements could be made on another material with a known radiation response using these same gauges and bonding agents, and comparisons made between known and measured responses.

Of the 19 samples studied, 68% of the samples' measured strain did not match the calculated thermal expansion of either the aluminum frame or the laminate. An example of measured strain inconsistent with calculated thermal expansion is shown in Fig. 8 with BF-CF-3 during Exposure 1. However, 21% of the measured strain of the sample corresponded with the thermal expansion calculation of the aluminum frame and 11% of the samples' measured strain matched the calculated thermal expansion of the laminate. An example of the measured strain matching the calculated thermal expansion of the aluminum frame is shown in Fig. 9 with CF-12 during Exposure 2. Fig. 10 presents the percent error between the measured strain and the calculated thermal expansion of the aluminum frame for CF-12. As shown in

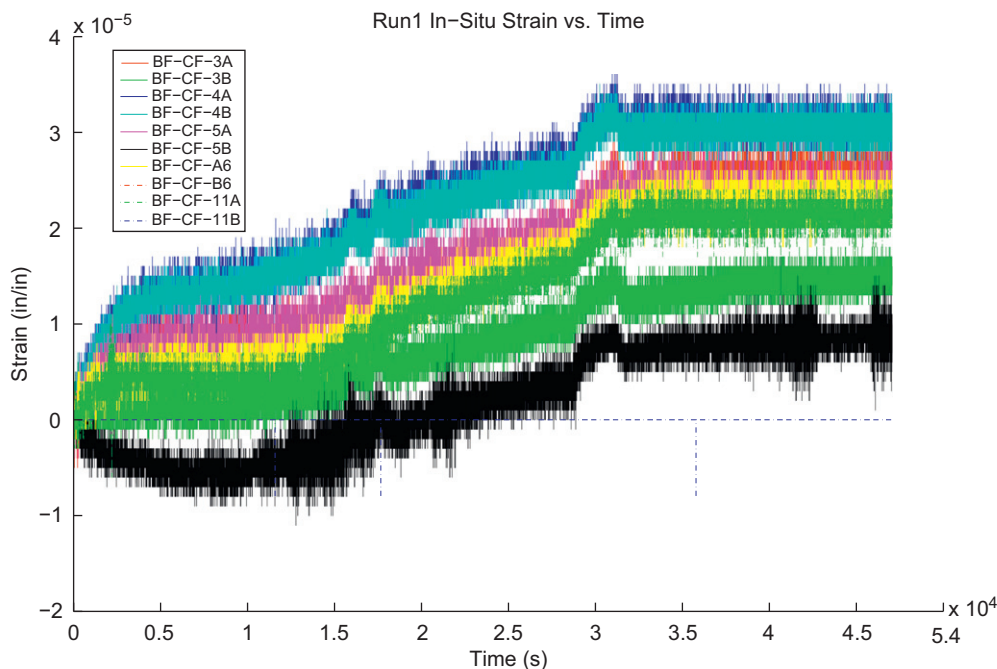


Fig. 6. Measured strain data from Exposure 1, example of a slow dose rate in-situ strain response.

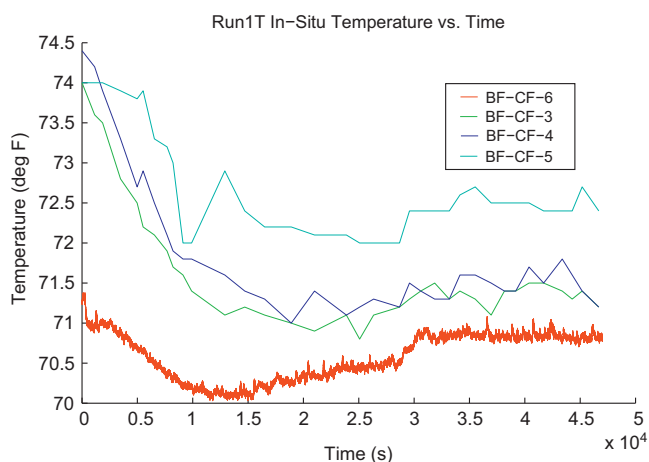


Fig. 7. Measured temperature data from Exposure 1.

the figure, initially there is significant error between the two. However, the error quickly declines throughout the remainder of the exposure. In addition, Fig. 11 displays an example of the measured strain of BF-CF-9 matching the calculated thermal expansion of the laminate. The corresponding percent error between the measured data and calculated expansion is given in Fig. 12. In the case of BF-CF-9, there is more error apparent between the comparison of the measured strain data and the calculated thermal expansion of the laminate. Given that a majority of the samples were not equivalent to the calculated thermal expansion for the aluminum frame or the laminate, and those samples that seemed to agree still contained some error in the comparison, demonstrates that the strain changes in the samples are a result of the radiation affecting the material.

Potential mechanisms responsible for the observed material behavior have been considered through comparison with the literature. Chain scission and crosslinking occur upon exposure of polymeric materials to radiation (Al-Sheikhly and Christou, 1994; O'Donnell et al., 1977; Otaguro et al., 2010; Coulter et al., 1986). Generally, these two mechanisms occur simultaneously,

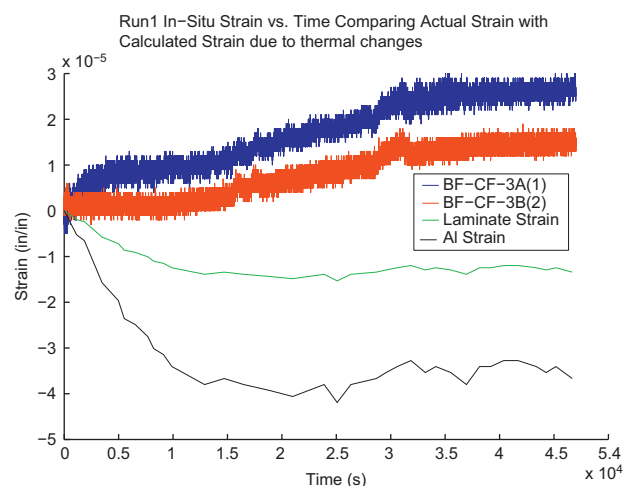


Fig. 8. An example (BF-CF-3) of measured strain overlaid with calculated thermal expansion of the aluminum frame and the BF-CF-epoxy material sample. This figure shows an example of a sample's measured strain that did not match the calculated thermal expansion of either the aluminum frame or the laminate.

with one predominating over the other. Crosslinking typically results in increased strength, increased average molecular weight, and embrittlement of the matrix, whereas chain scission results in decreased strength, decreased molecular weight, and degradation of the matrix (i.e., ductility). Comparing the outcome of these two mechanisms with the measured strain data during the radiation exposure suggests that with a fast dose rate exposure, the materials are shrinking as a result of enhanced matrix crosslinking. However, with a slow dose rate exposure, the samples are stretching, suggesting a possible degradation of the matrix through scission. A similar observation was reported in a study by Gillen and Clough (1981b), where dose rate effects existed for four different materials. The study concluded that scission effects became more important as the dose rate decreased, and that oxidative degradation was a possible explanation for the scission dominance at decreased dose rates. Other studies (Briskman et al.,

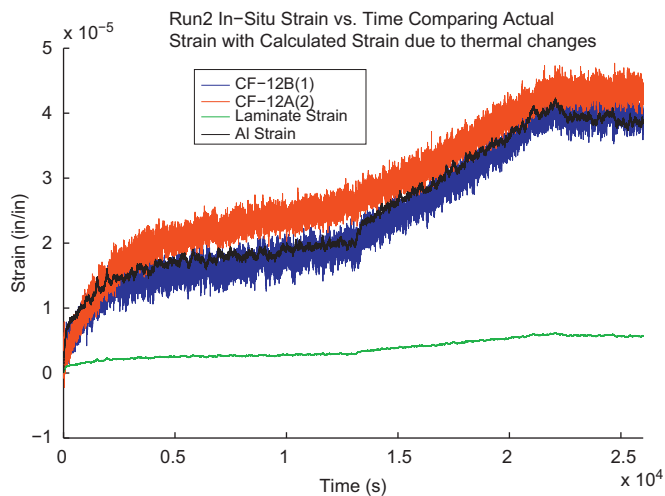


Fig. 9. An example (CF-12) of measured strain matching the calculated thermal expansion of the aluminum frame.

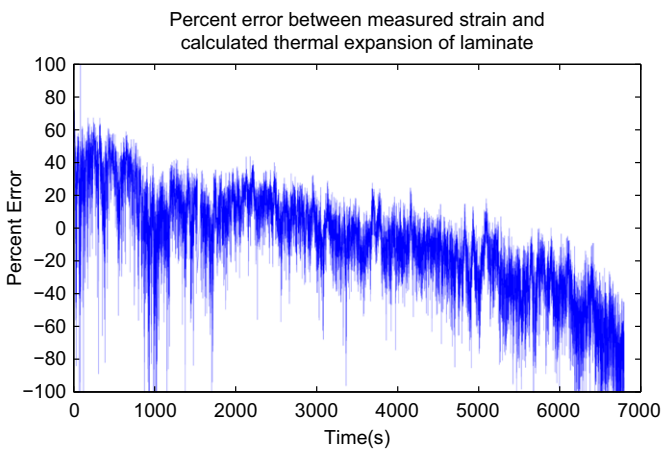


Fig. 12. The percent error between the measured strain and the calculated thermal expansion of the laminate for BF-CF-9.

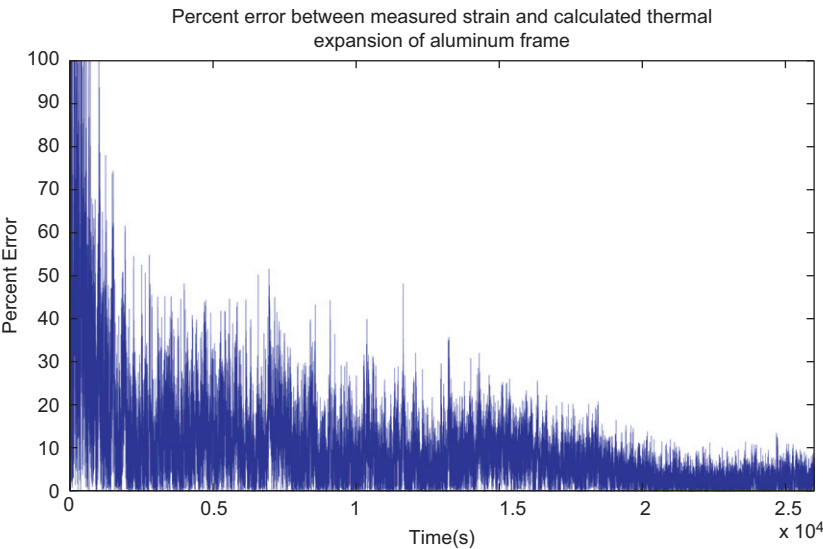


Fig. 10. The percent error between the measured strain and the calculated thermal expansion of the aluminum frame for CF-12.

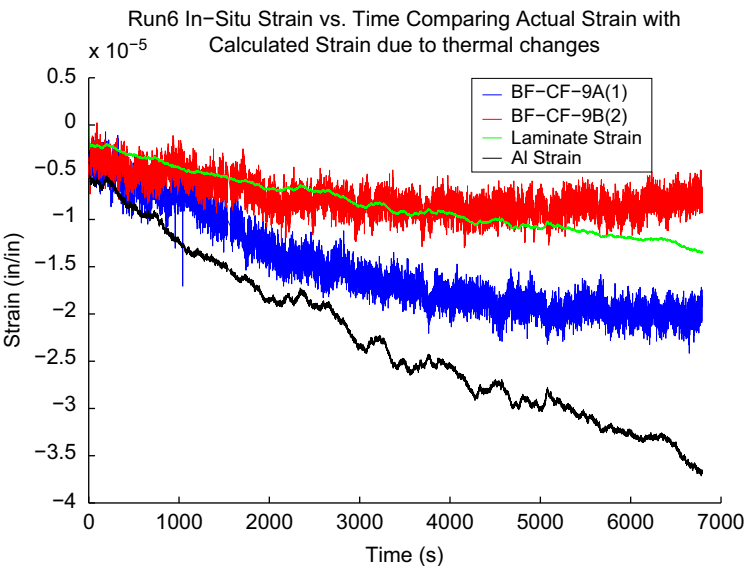


Fig. 11. An example (BF-CF-9) of measured strain matching the calculated thermal expansion of the laminate.

2004; Gillen and Clough, 1981a 1989; Sasuga et al., 1985; Seguchi et al., 1981) have also reported similar findings of scission-related effects due to oxidation at low dose rates. Given that the current study was performed in air at two extreme dose rates, the strain results suggest that oxidative degradation is the dominant degradation mechanism in the slow dose rate samples, giving rise to the increased strain behavior. Further characterization of these materials will be required to validate these assertions.

5. Summary and conclusions

Two composite materials were evaluated in a long-term radiation environment at two different dose rates. These materials were subjected to a simulated pressure stress while being exposed to radiation, and the strain of the materials was recorded. Exposure to a fast dose rate (0.1478 krad/s) produced a decrease in strain as a result of matrix shrinkage, and exposure to a slow dose rate (0.0139 krad/s) produced an increase in strain as a result of matrix stretching. We also concluded that the strain changes observed in the samples resulted from radiation exposure, and not from thermally induced strain changes. Finally, investigating previous studies of radiation exposed polymeric materials showed scission dominated effects as a result of oxidative degradation in polymers exposed to a decreased radiation dose rate in air. The measured results were compared with these studies to show potential mechanisms.

Acknowledgements

The authors would like to acknowledge the guidance and resources provided by NASA's Materials and Processes branch in the development and analysis of this study, in particular those of

Bradley Files, Steven Koontz, and John Alred. In addition, we would like to thank the Avionics System Division for their support with the irradiation of samples and data collection hardware borrowed for this study.

References

- Al-Sheikhly, M., Christou, A., 1994. Tutorial: how radiation affects polymeric materials. *IEEE Trans. Rel.* 43 (4), 551–556.
- Briskman, B.A., Klinshpont, E.R., Stepanov, V.F., Tlebaev, K.B., 2004. Determination of dose rate effects in polymers irradiated in vacuum. *J. Spacecraft Rockets* 41 (3), 360–365.
- Coulter, D.R., Gupta, A., Smith, M.V., Fornes, R.E., 1986. The Effects of Energetic Proton Bombardment on Polymeric Materials: Experimental Studies and Degradation Models. JPL Publication 85-101.
- Dorsey, J.T., Wu, K.C., Smith, R., 2008. Structural definition and mass estimation of lunar surface habitats for the Lunar Architecture Team Phase 2 (LAT-2) Study. In: *Proceedings of the Earth and Space 2008*.
- Gillen, K.T., Clough, R.L., 1981a. Radiation-thermal degradation of PE and PVC: mechanism of synergism and dose rate effects. *Radiat. Phys. Chem.* 18 (3–4), 661–669.
- Gillen, K.T., Clough, R.L., 1981b. Occurrence and implications of radiation dose-rate effects for material aging studies. *Radiat. Phys. Chem.* 18 (3–4), 679–687.
- Gillen, K.T., Clough, R.L., 1989. Time-temperature-dose rate superposition: a methodology for extrapolating accelerated radiation aging data to low dose rate conditions. *Polym. Degrad. Stabil.* 24, 137–168.
- Jablonski, A.M., Ogden, K.A., 2008. Technical requirements for lunar structures. *J. Aerospace Eng.* 2, 72.
- NASA-STD-3000, 1995. Man-Systems Integration Standards. Rev B 1 (5).
- O'Donnell, J.H., Rahman, N.P., Winzor, D.J., 1977. Evidence of crosslinking and chain scission in the degradation of poly(tert-butyl crotonate) by γ -irradiation. *J. Polym. Sci. Pol. Chem.* 15, 131–139.
- Otaguro, H., de Lima, L.F.C.P., Parra, D.F., Lugao, A.B., Chinelatto, M.A., Canevarolo, S.V., 2010. High-energy radiation forming chain scission and branching in polypropylene. *Radiat. Phys. Chem.* 79, 318–324.
- Sasuga, T., Hayakawa, N., Yoshida, K., Hagiwara, M., 1985. Degradation in tensile properties of aromatic polymers by electron beam irradiation. *Polymer* 26, 1039–1045.
- Seguchi, T., Arakawa, K., Hayakawa, N., Machi, S., 1981. Radiation induced oxidative degradation of polymers—IV. Dose rate effects on chemical and mechanical properties. *Radiat. Phys. Chem.* 18 (3–4), 671–678.